Review

The Andromeda Galaxy and its Star Formation History

Denis Leahy *

Posted Date: 15 May 2023

doi: 10.20944/preprints202305.0973.v1

Keywords: spiral galaxies; star formation; galactic structure; galaxy formation

Review

The Andromeda Galaxy and Its Star Formation History

Denis Leahy [1,*]

[1] Department of Physics and Astronomy, University of Calgary, Calgary Canada T2N 1N4; leahy@ucalgary.ca

* Correspondence: leahy@ucalgary.ca

Abstract: The state of knowledge of properties of the Andromeda Galaxy (also known as M31) is reviewed. The spatial structure of the Andromeda Galaxy, its main source populations and the properties of its gas and dust are discussed. To understand the formation history of the Andromeda Galaxy, the critical issues of its star formation history and the gas streams and dwarf galaxies in its surrounding environment are reviewed. Emphasis is on recent studies with important earlier work described in the references provided here. It is important to understand the Andromeda Galaxy because it is the nearest large external galaxy and is close enough for high resolution studies. This allows the Andromeda Galaxy to be used as a template to understand more distant and less resolved galaxies in the universe.

Keywords: spiral galaxies; star formation; galactic structure; galaxy formation

1. Introduction

Star formation histories of galaxies are critically important to understand the process of galaxy formation and the structure and contents of galaxies. Star formation can and has been studied in local galaxies for which the stellar populations and structural components of a galaxy are resolved. The structural components include those long recognized such as bulge, disk and halo. More recently recognized structures include separation of disks into thin and thick disk components and stellar streams. The latter are the most recently recognized, mainly using observations of the Milky Way and the Andromeda Galaxy (M31).

In this review, the properties of Andromeda/M31 are reviewed including its star formation history, which informs us on the galaxy's formation history. A recent study [1] focusses on the star formation history of 36 nearby (distance < 4 Mpc) dwarf galaxies and concludes that the local volume dwarf galaxies are consistent with a synchronized star formation history. Another study of local group galaxies [2] considers the dust emission (100 to 500 micron wavelengths) which is related to star formation because young stars are the primary heating source of the dust.

We focus on M31 because it is the nearest large spiral galaxy to the Milky Way, and it has several advantages over Milky Way studies. These include the unobscured view because we do not need to look through the dust of the Milky Way disk, the known distances to M31 stars and other objects, and the global view of M31 which is not confused like our inside view of the Milky Way.

M31 is also of interest because it is the most massive member of the local group with the Milky Way as the only other massive galaxy. Using Gaia data [3], the motion of M31 relative to the Milky Way was determined better than previously, confirming that the two massive galaxies are infalling toward their first close encounter.

Other related properties of M31 in addition to direct measures of star formation history are mentioned here. These include the structure of the galaxy, including bulge, disk, halo, and stellar streams. Because high resolution ultraviolet (UV) observations have recently become available, UV measures of M31's star formation and galaxy structure are emphasized.

Preprints (www.preprints.org) | NOT PEER-REVIEWED | Posted: 15 May 2023 doi:10.20944/preprints202305.0973.v1

M31 is a giant spiral galaxy similar to the Milky Way but with roughly twice the mass. The galaxy's spiral structure is clearly seen in optical images (e.g. Figure 1) as are prominent dust lanes, especially NW of the central bulge. That the dust lanes are visible in the NW but not in the SE is a clear indicator that the NW disk is in front of the bulge and the SE disk is behind the bulge. I.e. the M31 rotation axis is tilted away from the observer in the NW and toward the observer in the SE. In Figure 1 are also seen two neighboring dwarf galaxies: NGC205 is NE of the bulge, just right of field F5, and M32 is in field F6, just west of center of that field.

For this review of M31, the areas of study are divided into 5 general topics. Section 2 discusses the structure of M31, and Section 3 lists the source populations in M31. Section 4 discusses the gas and dust in M31 and section 5 describes what we know about the star formation history of M31. Section 6 discussed the environment of M31. By necessity this review is not complete but focusses on work since about 2015, with the earlier work discussed in the provided references.

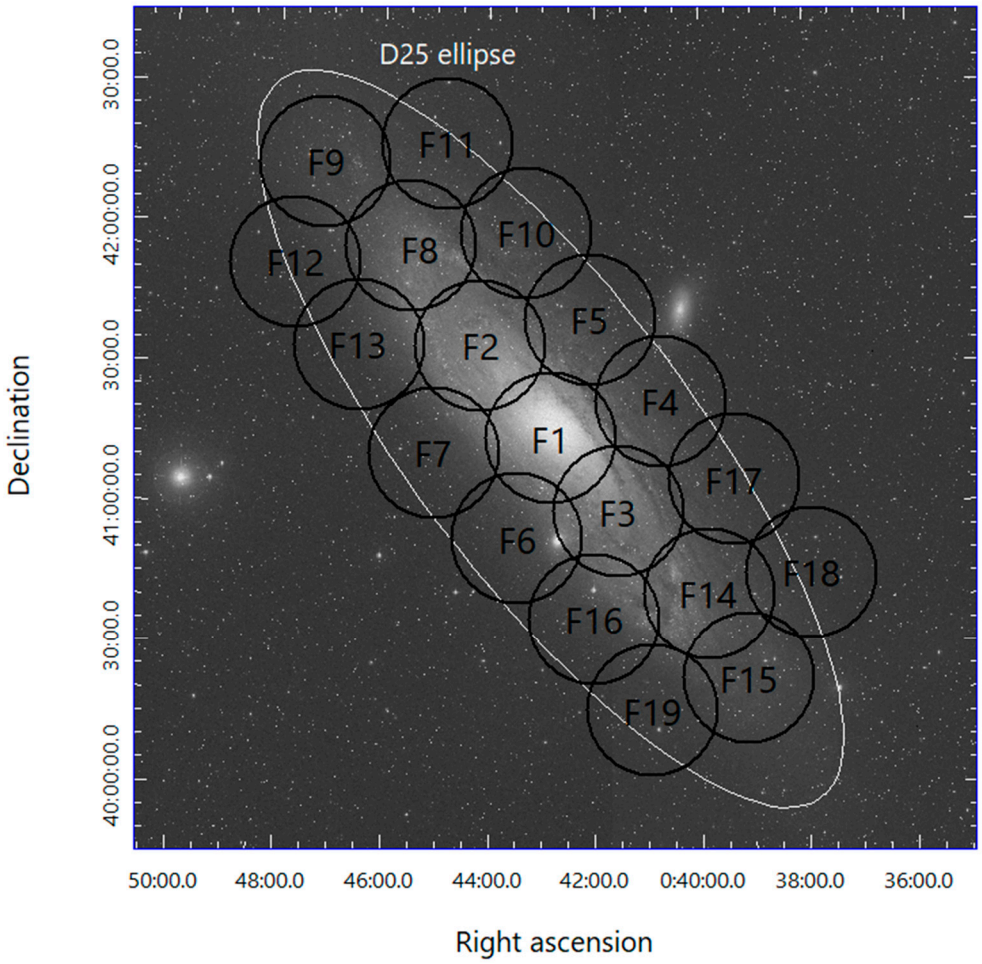

Figure 1. The greyscale image is the DSS Poss2 blue filter image of M31. Right ascension and declination are J2000 coordinates. The white ellipse shows the D25 ellipse for M31, from [4]. The locations of the fields, F1 to F19, for the UVIT survey of M31, are shown by the black circles (from [5]).

2. Structure of M31

M31 is an SAb type spiral galaxy (see https://ned.ipac.caltech.edu) with luminosity in the visible band of 3×10^{11} solar luminosities. It has near infrared at 1/3 of that, and far infrared and ultraviolet luminosities about 1/30 and 1/60 of the visible band luminosity. The visible band image is shown in Figure 1 and is dominated by light from older stars, with some prominent lanes caused by absorption by dust in the interstellar medium. The ultraviolet and far infrared images are shown in Figure 2 (left and right panels, respectively). Both images are dominated by the spiral arms, but for different

Preprints (www.preprints.org) | NOT PEER-REVIEWED | Posted: 15 May 2023 doi:10.20944/preprints202305.0973.v1

reasons: the hot young stars in the spiral arms dominate the ultraviolet emission, whereas the far infrared is from the interstellar dust around the hot stars (and heated by those hot stars). The far infrared luminosity is larger than the ultraviolet luminosity because only a small fraction of the luminosity of the hot stars is in the ultraviolet band whereas most of the luminosity is converted to far infrared radiation by the dust.

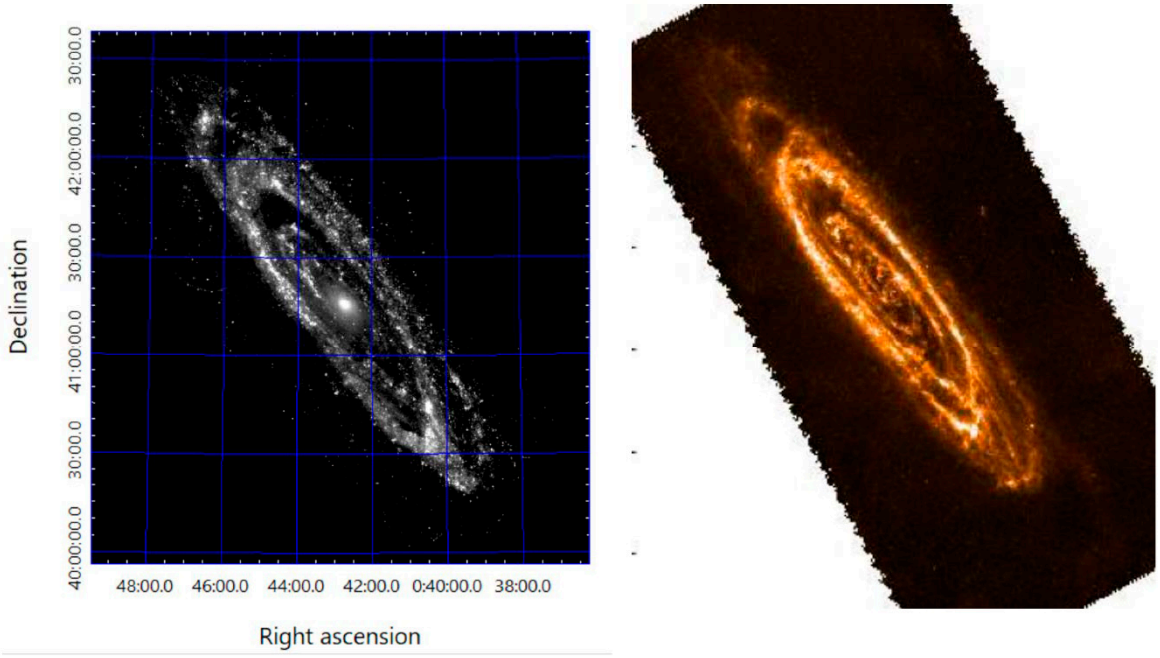

Figure 2. Images of M31 at ultraviolet and infrared wavelengths. (**a**) The 148 nm image of M31 [6]. (**b**) (b) The far infrared 250 micron image of M31 from the Hershel SPIRE instrument [7]. The ultraviolet and far infrared images closely trace the spiral arms of M31.

The major structures for spiral galaxies are present in M31: the disk, the central bulge and the halo. The luminosity profile of M31 in near-infrared (sensitive to stars and insensitive to dust) was modeled by [8] with the above 3 components. The main parameters were a disk scale length of 5.3 kpc, a bulge Sersic-function index of 2.2 and effective radius of 1 kpc, a halo with power-law profile with index -2.5. The kinematics of the disk stars and gas were analyzed by [9], showing that the offset in stellar and gas velocity increases with stellar age. They find that a simple tilted ring model to explain the warps in the disk is inadequate.

The bulge is known to be triaxial and has been analyzed using N-body simulations [10]. To match the bulge properties an initial classical bulge (which is formed by violent relaxation early in the formation of the galaxy) with 1/3 of the total bulge mass and a Box/Peanut bulge with 2/3 of the total bulge mass are required. The structure of the bulge was analyzed in ultraviolet by [11]. The bulge was found to be complex with a boxy shape and found to require an 8-component model: 3 Sersic-function models for the main bulge and 5 components for the inner bulge and nuclear region.

At the very center of M31 (radius < 4pc) there is a nuclear stellar disk orbiting the supermassive black hole [12], with a disk precession rate consistent with disk stellar winds driving the accretion into the central region.

3. Source populations in M31

M31 contains several populations, including point-like ones (stars, X-ray sources), and extended ones (globular and open clusters, planetary nebulae and supernova remnants). A number of star catalogs for M31 have been assembled (e.g. see references in [13]). The largest is from the

 doi:10.20944/preprints202305.0973.v1

Panchromatic Hubble Andromeda Treasury (PHAT), presented by [13] with 117 million stars. An ultraviolet catalog of sources in M31 was presented by [5] with ~80000 sources. Far ultraviolet variable stars were found by [14,15] using multi-epoch observations and identified with hot young stars.

373 X-ray sources and optical counterparts for half of them were studied by [16]. Half of the counterparts are background galaxies, the other falling into several categories including foreground stars, star clusters and supernova remnants. The main problem with identifying optical counterparts is the intrinsic faintness of the X-ray sources in optical. Ref. [17] identified 15 high-mass X-ray binaries and found that they are located in regions with young stars (less than 50 Myr old). Ultraviolet counterparts for 67 X-ray sources in M31 were found by [18] with the largest population being globular clusters. For the globular clusters the ultraviolet emission was from blue horizontal branch stars in the cluster, whereas the X-ray emission was from an X-ray binary in the cluster.

The globular clusters are the oldest stellar populations and were found to consist of 3 major groups [19]: (1) an inner metal-rich group ([Fe/H] > -0.4); (2) a group with intermediate metallicity (with median [Fe/H] = −1); and (3) a metal-poor group, with [Fe/H] < -1.5. Here [Fe/H] is the log of the metal abundance (in this case iron) relative to that for the Sun. The metal-rich group has kinematics and spatial properties like those of the disk of M31, while the two more metal-poor groups show mild prograde rotation overall.

Supernova remnants in M31 have been studied in a number of works ([6,20] and references therein). The number of supernova remnants (180) is dominated by those discovered in optical emission lines, with 26 detected in X-rays [20]. The positions of the supernova remnants are closely associated with the spiral arms of M31 [6], which is expected because of the short lifetime of supernova remnants (~50,000 yr) and that ¾ of them are from massive star explosions. For the Milky Way this association is not possible to see because of the distance uncertainties of the supernova remnants.

Planetary nebulae are useful to trace the structure of the young thin disk and old thick disk of a galaxy, and their velocities can be used to trace the disk kinematics. For M31 [21,22] find that the thin disk and thick disk in M31 are 2 and 3 times as thick as the corresponding disks in the Milky Way. The age-velocity dispersion relation derived from planetary nebulae in M31 indicates that a major merger of M31 with a satellite of 1/5 the mass of M31 took place 2.5 to 4.5 Gyr ago.

4. Gas and dust in M31

The gas and dust components of M31 are significant: as with many spiral galaxies dark lanes in the disk are seen at optical wavelengths, caused by absorption by dust (Figure 1, northwest side of the disk). The neutral interstellar medium has been mapped in the 21 cm line of neutral hydrogen. The recent work of [23] uses high spatial resolution observations of M31 to find that spectra for most lines-of-sight are better fit by multi-component Gaussian lineshapes, and that studies of the opaque component of the neutral gas are best constrained by absorption studies.

Far infrared maps were analyzed by [2] to determine dust mass, temperature, and luminosity maps for M31 and compare it to maps for M33 and the Large and Small Magellanic Clouds. Dust temperature and surface density were found to be higher for star forming regions. By degrading the spatial resolution to mimic observations of more distant galaxies, they found that the temperature is systematically overestimated and the dust mass underestimated for the more distant galaxies.

The dust distribution in the central bulge (radius < 700 pc) of M31 was mapped by [24] using near ultraviolet to near infrared high resolution imaging. The dust clumps are mostly located in a plane which is roughly face-on. For supernova remnants in M31, the dust temperature and mass were derived from fitting the near to far infrared spectral energy distributions. The dust surface density in supernova remnants was found to be half that in the surrounding regions, implying dust destruction by the supernova explosion.

Radiative transfer simulations to study the dust extinction in M31 were carried out by [25]. They reproduce the morphology and flux density from ultraviolet to sub-millimeter wavelengths,

 doi:10.20944/preprints202305.0973.v1

obtaining an attenuation curve consistent with previous estimates and find that 90% of the heating of the dust is caused by evolved stellar populations.

5. Star formation history of M31

The star formation history of M31 has been studied extensively, in large part because of the spatial resolution attainable: a typical resolution of 1 arcsecond is 3.8 pc at the distance of M31, and Hubble Space Telescope (HST) observations have 10 times finer resolution. Ref. [26] carried out a color–magnitude diagram (CMD) analysis of HST-resolved stars. This included both open clusters and field stars in part of the northeast disk of M31, with an upper age limit of ~300 Myr. The cluster formation efficiency was found to vary across the disk, consistent with variations in mid-plane pressure. Models for cluster formation efficiency better reproduced observations when the gas depletion timescale was different for neutral hydrogen and molecular hydrogen dominated environments.

Ref. [27] developed the method of pixel CMD analysis to take into account partially resolved stellar populations and to be able to study the crowded bulk and disk regions of M31. Using 7 age bins from 10^6 to 10^{10} yr, they find a smooth exponential decay in star formation rate for the disk with timescale 4 Gyr and for the bulge with 2 Gyr timescale. Ref. [28] derive age, mass and extinction for 1363 star clusters in M31 observed with HST. They found that the mass function of clusters is compatible with mass functions found in other spiral galaxies, and it follows a Schecter function with characteristic mass of 10^5 Solar masses. Ref. [29] measured the star formation history using HST observations of the northeast disk of M31. They fit CMDs to a large number of small regions (0.3 kpc by 1.4 kpc) and find that most stars form prior to 8 Gyr ago, followed a relatively quiet period until 4 Gyr ago, with another star formation episode 2 Gyr ago, followed by recent quiescence.

The star formation history of the bulge of M31 was studied by [30] using HST CMDs. They find the that more than 70 per cent of the stars in the bulge are old (>5 Gyr) and metal rich ([Fe/H] ~ 0.3). At about 1 Gyr ago there was a significant rise in star formation over the entire bulge region. For the central 130 arcsec (400 pc) there was an additional star formation episode <500 Myr old. Ref. [31] derived stellar population properties using Lick/IDS absorption line indices. The classical central bulge (<100 arcsec) was found to be old (11-13 Gyr) and metal rich ([Fe/H] ~0.3). The bar (extending out to 600 arcsec) is distinct in metallicity with near solar metallicity. The boxy-peanut component of the bulge also has near solar metallicity. The mass-to-light ratio of the above 3 components is the same, at 4.5 solar mass per solar luminosity. The disk of M31 (800 to 1600 arcsec from center) includes a mixture of ages with youngest at ~3-4 Gyr and with mass-to-light ratio of 3 solar mass per solar luminosity.

Star formation studies of the bulge and disk were carried out using far ultraviolet observations from the UVIT instrument with the method of spectral energy distribution fitting. Ultraviolet observations are particularly sensitive to the youngest stars. Ref. [33] verified the result from [30] that the innermost bulge (100 arcsec) has a young stellar component of age ~100 Myr, and a more recent star formation peak. Inclusion of broader band data (near and far infrared) in the SED fits gave improved results [34]: the bulge was found to have a dominant old (10–12 Gyr) metal-rich ([Z/H] ~ 0.3) population and a younger (600 Myr) solar abundance ([Z/H] ~ 0) population throughout. For the innermost 120 arcsec a very young (25 Myr) metal-poor ([Z/H]~−0.7) populations was found. For the disk of M31 [32], 239 clusters in the northeast disk and bulge were modeled to measure ages, masses, metallicities and extinctions. Figure 3 (left panel) shows the locations of the clusters, with their ages indicated by the symbol size and color. Figure 3 (right panel) shows the ages of the clusters vs. deprojected distance from the center of M31. The bulge has the oldest clusters, and the disk contains a mixture of two age groups: one about 100 Myr old and a second about 4 Myr old.

Preprints (www.preprints.org) | NOT PEER-REVIEWED | Posted: 15 May 2023 doi:10.20944/preprints202305.0973.v1

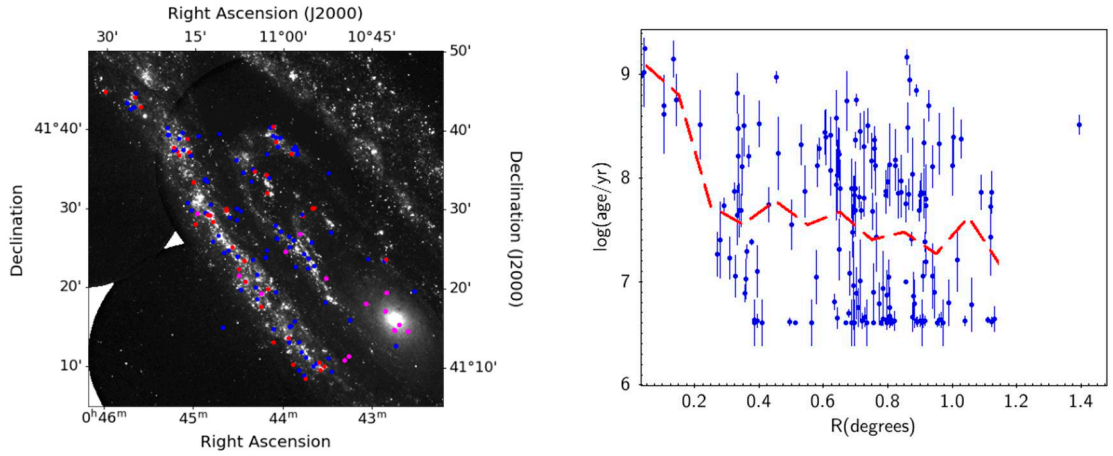

Figure 3. (**a**) Positions and ages of the clusters in the northeast disk and bulge of M31 studied by [34]. Log(age/yr) values are shown by the size of the circles with radius proportional to log(age/yr) and total range 6.6 to 9.7. Clusters with log(age/yr) < 6.75 are plotted in red, 6.75 < log(age/yr) < 8.55 are shown in magenta. (**b**)). Log(age/yr) of each cluster vs deprojected distance from the center of M31 (blue symbols with error bars). The red dashed line shows the mean value for each bin.

6. Surrounding environment of M31

The standard picture of galaxy formation in an expanding universe includes a number of aspects, including early formation of density fluctuations. The scale and strength of the density fluctuations is derived from measurements of cosmic microwave background inhomogeneities. The density fluctuations result in formation of the first mass concentrations and the first stars. The continued growth of the amplitude of density fluctuations results in formation of the filamentary cosmic web, followed by the formation of large mass concentrations and galaxies at the intersection of filaments. Galaxies continue to grow as matter flows along the filaments onto the mass concentrations.

Various processes related to the growth and assembly of M31 have been studied by observing the surrounding environment of the galaxy. Here, recent work is summarized. Ref. [35] fits red giant branch stars in color-magnitude space to study M31's giant stellar stream and streams C and D. The metallicity of the stars for the giant stellar stream increases from -0.7 to -0.2 outward with distance from M31. Ref. [36] use data from the Pan-Andromeda Archaeological Survey which covers >400 degree^2. They find that the 13 most distinctive substructures were produced by at least 5 different accretion events, all in the last 3 or 4 Gyr. The OPTICS clustering algorithm is used to quantify the hierarchical structure of M31's stellar halo and identify three new faint structures. The newer work by [37] using spectroscopy did not confirm a metallicity, measured by [α/Fe] in the giant stellar stream, but found a high [α/Fe] in the outer disk of M31, which is characteristic of rapid star formation induced by a major merger.

Simulations of M31 were carried out by [38] to explain recent observations that imply the disk was shaped by significant events during 2-4 Gyr ago. The simulations lead to the conclusion that most of the halo substructure and complexity in the inner part of M31 can be caused by a single major interaction, for which the interacting galaxy has now merged with M31.

The circum-galactic medium (CGM) of M31 was studied by [39] using absorption line spectroscopy for 43 sightlines to background QSOs with impact parameters of 25 to 570 kpc. The covering factor of Si III and O VI absorption lines is near unity, showing that M31 has an extended ionized CGM (T~10^4 – $10^{5.5}$ K). The Milky Way likely has a similarly extended CGM which extends far enough to overlap that of M31.

This review ends with a discussion of the satellite system of M31. The mass, metallicity and velocity dispersion for 256 stars in 5 dwarf spheroidal satellites were derived from Keck spectroscopy by [40]. They show that M31 and Milky Way satellites obey the same relation between mass and

metallicity. The M31 dwarf spheroidal galaxies are more metal poor than the giant stellar stream or the smooth inner halo. This is consistent with the inner halo being the surviving remnants of more massive satellites that merged with M31 early in its history.

The missing satellites problem was studied using cosmological hydrodynamic models by [41]. At a fixed host mass of 10^{12} solar masses, the simulations find a wide range of numbers of satellites. The number of satellites accreted is larger than number of surviving satellites by a factor of 4-5. Thus they find there is no missing satellites problem. The satellites in the local group are known to be located to within ~30 degrees of a plane. Ref. [42] carried out cosmological simulations for Milky Way and M31 mass hosts to estimate the frequency of satellite positions that are near to a plane. They conclude that the coincidence of satellites lying near a plane is high enough that there is no plane-of-satellites problem.

7. Summary

In this review, the state of knowledge of the Andromeda Galaxy (M31) has been discussed, including its structure, source populations, gas and dust contents, star formation history and surrounding environment. An understanding of M31 is important because it is the nearest large galaxy to us, outside the Milky Way, and is amenable to detailed studies which allow it to be used as a template to understand more distant and difficult to observe galaxies in the universe.

Funding: This research was funded by the Canadian Space Agency, grant number 10036281.

Data Availability Statement: No new data were created or analyzed in this review article. Data sharing is not applicable to this article.

Conflicts of Interest: The author declares no conflict of interest. The funders had no role in the design of the study; in the collection, analyses, or interpretation of data; in the writing of the manuscript; or in the decision to publish the results.

References

1. Olsen, C.; Gawiser, E.; Iyer, K. et al. Star Formation Histories from Spectral Energy Distributions and Color-magnitude Diagrams Agree: Evidence for Synchronized Star Formation in Local Volume Dwarf Galaxies over the Past 3 Gyr. *The Astrophysical Journal* **2021**, *913*, id.45. DOI: 10.3847/1538-4357/abf3c2
2. Utomo, D.; Chiang, I.; Leroy, A. et al. The Resolved Distributions of Dust Mass and Temperature in Local Group Galaxies. *The Astrophysical Journal* **2019**, *874*, id.141. DOI: 10.3847/1538-4357/ab05d3
3. van der Marel, R.; Fardal, M.; Sohn, S. et al. First Gaia Dynamics of the Andromeda System: DR2 Proper Motions, Orbits, and Rotation of M31 and M33. *The Astrophysical Journal* **2019**, *872*, id.24. DOI: 10.3847/1538-4357/ab001b
4. Gil de Paz, A.; Boissier, S.; Madore, B. et al. The GALEX Ultraviolet Atlas of Nearby Galaxies. *The Astrophysical Journal Supplement Series* **2007**, *173*, pp. 185-255. DOI: 10.1086/516636
5. Leahy, D.; Postma, J.; Chen, Y.; Buick, M. AstroSat UVIT Survey of M31: Point-source Catalog. *The Astrophysical Journal Supplement Series* **2020**, *247*, id.47. DOI: 10.3847/1538-4365/ab77a9
6. Leahy, D.; Monaghan, C.; Ranasinghe, S. Discovery of 20 UV-emitting SNRs in M31 with UVIT. *The Astronomical Journal* **2023**, *165*, id.116. DOI: 10.3847/1538-3881/acb68d
7. Herschel Data Search. Available online: https://irsa.ipac.caltech.edu/applications/Herschel/ (accessed on 14-05-2023 Year).
8. Courteau, S.; Widrow, L.; McDonald, M. et al. The Luminosity Profile and Structural Parameters of the Andromeda Galaxy. *The Astrophysical Journal* **2011**, *739*, id.20. DOI: 10.1088/0004-637X/739/1/20
9. Quirk, A.; Guhathakurta, P.; Chemin, L. et al. Asymmetric Drift in the Andromeda Galaxy (M31) as a Function of Stellar Age. *The Astrophysical Journal* **2019**, *871*, id.11. DOI: 10.3847/1538-4357/aaf1ba
10. Blana Dıaz, M., Wegg, C; Ortwin, G. et al. Andromeda chained to the box - dynamical models for M31: bulge and bar. *Monthly Notices of the Royal Astronomical Society* **2017**, *466*, p.4279-4298. DOI: 10.1093/mnras/stw3294
11. Leahy, D.; Craiciu, T., Postma, J. The Complex Structure of the Bulge of M31. *The Astrophysical Journal Supplement Series* **2023**, *265*, id.6. DOI: 10.3847/1538-4365/acae90

12. Lockhart, K.; Lu, J.; Peiris, H. et al. A Slowly Precessing Disk in the Nucleus of M31 as the Feeding Mechanism for a Central Starburst. *The Astrophysical Journal* **2018**, *854*, id.121. DOI: 10.3847/1538-4357/aaaa71
13. Williams, B.; Lang, D.; Dalcanton, J. The Panchromatic Hubble Andromeda Treasury. X. Ultraviolet to Infrared Photometry of 117 Million Equidistant Stars. *The Astrophysical Journal Supplement Series* **2014**, *215*, id.9. DOI: 10.1088/0067-0049/215/1/9
14. Leahy, D.; Buick, M.; Postma, J. et al. Far-ultraviolet Variable Sources in M31. *The Astronomical Journal* **2021**, *161*, id.215. DOI: 10.3847/1538-3881/abe9b3
15. Leahy, D.; Buick, M.; Postma, J. Far-ultraviolet Variables in M31: Concentration in Spiral Arms and Association with Young Stars. *The Astronomical Journal* **2021**, *162*, id.199. DOI: 10.3847/1538-3881/ac1e93
16. Williams, B.; Lazzarini, M.; Plucinsky, P. Comparing Chandra and Hubble in the Northern Disk of M31. *The Astrophysical Journal Supplement Series* **2018**, *239*, id.13. DOI: 10.3847/1538-4365/aae37d
17. Lazzarini, M.; Hornschemeier, A.; Williams, B. Young Accreting Compact Objects in M31: The Combined Power of NuSTAR, Chandra, and Hubble. *The Astrophysical Journal* **2018**, *862*, id.28. DOI: 10.3847/1538-4357/aacb2a
18. Leahy, D.; Chen, Y. AstroSat UVIT Detections of Chandra X-Ray Sources in M31. *The Astrophysical Journal Supplement Series* **2020**, *250*, id.23. DOI: 10.3847/1538-4365/abadfb
19. Caldwell, N.; Romanowsky, A. Star Clusters in M31. VII. Global Kinematics and Metallicity Subpopulations of the Globular Clusters. *The Astrophysical Journal* **2016**, *824*, id.42. DOI: 10.3847/0004-637X/824/1/42
20. Sasaki, M.; Pietsch, W.; Haberl, F. et al. Supernova remnants and candidates detected in the XMM-Newton M 31 large survey. *Astronomy & Astrophysics* **2012**, *544*, id.A144. DOI: 10.1051/0004-6361/201219025
21. Bhattacharya, S.; Arnaboldi, M.; Hartke, J. et al. The survey of planetary nebulae in Andromeda (M 31). I. Imaging the disc and halo with MegaCam at the CFHT. *Astronomy & Astrophysics* **2019**, *624*, id.A132. DOI: 10.1051/0004-6361/201834579
22. Bhattacharya, S.; Arnaboldi, M.; Caldwell, N. et al. The survey of planetary nebulae in Andromeda (M 31). II. Age-velocity dispersion relation in the disc from planetary nebulae. *Astronomy & Astrophysics* **2019**, *631*, id.A56. DOI: 10.1051/0004-6361/201935898
23. Koch, E.; Rosolowsky, E.; Leroy, A. et al. A lack of constraints on the cold opaque H I mass: H I spectra in M31 and M33 prefer multicomponent models over a single cold opaque component. *Monthly Notices of the Royal Astronomical Society* **2021**, *504*, p.1801-1824. DOI: 10.1093/mnras/stab981
24. Dong, H.; Li, Z.; Wang, Q. et al. High-resolution mapping of dust via extinction in the M31 bulge. *Monthly Notices of the Royal Astronomical Society* **2016**, *459*, p.2262-2273. DOI: 10.1093/mnras/stw778
25. Viaene, S.; Baes, M.; Tamm, A. et al. The Herschel Exploitation of Local Galaxy Andromeda (HELGA). VII. A SKIRT radiative transfer model and insights on dust heating. *Astronomy & Astrophysics* **2017**, *599*, id.A64. DOI: 10.1051/0004-6361/201629251
26. Johnson, L.; Seth, A.; Dalcanton, J. Panchromatic Hubble Andromeda Treasury. XVI. Star Cluster Formation Efficiency and the Clustered Fraction of Young Stars. *The Astrophysical Journal* **2016**, *827*, id.33. DOI: 10.3847/0004-637X/827/1/33
27. Conroy, C.; van Dokkum, P. Pixel Color Magnitude Diagrams for Semi-resolved Stellar Populations: The Star Formation History of Regions within the Disk and Bulge of M31. *The Astrophysical Journal* **2016**, *827*, id.9. DOI: 10.3847/0004-637X/827/1/9
28. de Meulenaer, P.; Stonkutė, R.; Vansevičius, V. Deriving physical parameters of unresolved star clusters. V. M 31 PHAT star clusters. *Astronomy & Astrophysics* **2017**, *602*, id.A112. DOI: 10.1051/0004-6361/201730751
29. Williams, B.; Dolphin, A.; Dalcanton, J. et al. PHAT. XIX. The Ancient Star Formation History of the M31 Disk. *The Astrophysical Journal* **2017**, *846*, id.145. DOI: 10.3847/1538-4357/aa862a
30. Dong, H.; Olsen, K.; Lauer, T. et al. The star formation history in the M31 bulge. *Monthly Notices of the Royal Astronomical Society* **2018**, *478*, p.5379-5403. DOI: 10.1093/mnras/sty1381
31. Saglia, R.; Opitsch, M. ; Fabricius, M. et al. Stellar populations of the central region of M 31. *Astronomy & Astrophysics* **2018**, *618*, id.A156. DOI: 10.1051/0004-6361/201732517
32. Leahy, D.; Buick, M.; Leahy. C. AstroSat/UVIT Cluster Photometry in the Northern Disk of M31. *The Astronomical Journal* **2022**, *164*, id.183. DOI: 10.3847/1538-3881/ac9058

33. Leahy, D.; Morgan, C.; Postma, J.; Buick, M. ASTROSAT/UVIT Near and Far Ultraviolet Properties of the M31 Bulge. *International Journal of Astronomy and Astrophysics* **2021**, *11*, pp. 151-174. DOI: 10.4236/ijaa.2021.112009
34. Leahy, D.; Seminoff, N.; Leahy. C. Far-ultraviolet to FIR Spectral-energy Distribution Modeling of the Stellar Formation History of the M31 Bulge. *The Astronomical Journal* **2022**, *163*, id.138. DOI: 10.3847/1538-3881/ac4cca
35. Conn, A.; McMonigal, B.; Bate, N. et al. Major substructure in the M31 outer halo: distances and metallicities along the giant stellar stream. *Monthly Notices of the Royal Astronomical Society* **2016**, *458*, p.3282-3298. DOI: 10.1093/mnras/stw513
36. McConnachie, A.; Ibata, R.; Martin, N. et al. The Large-scale Structure of the Halo of the Andromeda Galaxy. II. Hierarchical Structure in the Pan-Andromeda Archaeological Survey. *The Astrophysical Journal* **2018**, *868*, id.55. DOI: 10.3847/1538-4357/aae8e7
37. Escala, I.; Gilbert, K.; Kirby, E. et al. Elemental Abundances in M31: A Comparative Analysis of Alpha and Iron Element Abundances in the the Outer Disk, Giant Stellar Stream, and Inner Halo of M31. *The Astrophysical Journal* **2020**, *889*, id.177. DOI: 10.3847/1538-4357/ab6659
38. Hammer, F.; Yang, Y.; Wang, J. et al. A 2-3 billion year old major merger paradigm for the Andromeda galaxy and its outskirts. *Monthly Notices of the Royal Astronomical Society* **2018**, *475*, p.2754-2767. DOI: 10.1093/mnras/stx3343
39. Lehner, N.; Berek, S.; Howk, J. et al. Project AMIGA: The Circumgalactic Medium of Andromeda. *The Astrophysical Journal* **2020**, *900*, id.9. DOI: 10.3847/1538-4357/aba49c
40. Kirby, E.; Gilbert, K.; Escala, I. et al. Elemental Abundances in M31: The Kinematics and Chemical Evolution of Dwarf Spheroidal Satellite Galaxies. *The Astronomical Journal* **2020**, *159*, id.46. DOI: 10.3847/1538-3881/ab5f0f
41. Engler, C.; Pillepich, A.; Pasquali, A. et al. The abundance of satellites around Milky Way- and M31-like galaxies with the TNG50 simulation: a matter of diversity. *Monthly Notices of the Royal Astronomical Society* **2021**, *507*, p.4211-4240. DOI: 10.1093/mnras/stab2437
42. Samuel, J.; Wetzel, A.; Chapman, S. et al. Planes of satellites around Milky Way/M31-mass galaxies in the FIRE simulations and comparisons with the Local Group. *Monthly Notices of the Royal Astronomical Society* **2021**, *504*, p.1379-1397. DOI: 10.1093/mnras/stab955